Preparation of Nano-Sized Chromium Clusters and Intimate Mixtures of Chromium/CdS Phases in a Porous Hybrid Xerogel by an Internal Doping Method

Kyung Moon Choi and Kenneth J. Shea*

Contribution from the Department of Chemistry, University of California, Irvine, California 92717-2025

Received May 25, 1994®

Abstract: A procedure for creating nano-sized chromium clusters (10–100 Å) in a porous amorphous hybrid xerogel is described. The xerogel, a poly(1,4-phenylene) bridged silsesquioxane, is a hybrid organic–inorganic network material prepared by sol–gel processing of 1,4-bis(triethoxysilyl)benzene (**M-1**) and chromium tricarbonyl (triethoxysilyl)-benzene (**M-2**). Chromium(0) metal clusters were produced by an *internal* doping procedure. Following drying, the hybrid xerogel, when heated to 120 °C under high vacuum, results in the formation of irregularly shaped, nano-sized chromium clusters. TEM images were used to establish the size of the metal particles. EDAX and electron diffraction techniques were used to verify the elemental composition and morphology of the metal clusters. Only a slight decrease in surface area and an increase in pore diameter were observed following chromium metal deposition. Intimately mixed nanophases consisting of CdS and chromium metal were also prepared by a combination of external and internal doping procedures.

Introduction

During the past decade, the preparation and characterization of nano-sized semiconductor particles and metal clusters have been an active area of investigation.[1-4] Nano-sized semiconductor and metal particles are composed of clusters containing from a few hundred to several thousand atoms or molecules. Aside from their very high surface area, these particles can possess chemical and physical properties that are distinct both from the bulk phase and from individual molecules.

Methodology has been developed for the preparation of nano-sized particles in a variety of materials including polymer films,[5] celluloses,[6] vesicles,[7] and glassy materials.[8-11] Nano-sized particles ranging in size from ten to hundreds of angstrom are being evaluated for applications in photochemistry,[12,13] electrochemistry,[14] and optics[15-17] and as catalysts.[18,19] Nano-sized particles also show interesting optical properties and their utilization in optical devices is receiving attention.[20,21] Nano-sized transition metal clusters are of enormous importance as catalysts in many industrial processes. Their methods of preparation and uses have been the subject of several articles. Recent examples include the preparation of nano-sized cobalt[22] and palladium[23] crystallites in glassy carbon matrices.

In this paper, we report novel technology for the preparation of nano-sized chromium clusters in a porous inorganic–organic xerogel. The materials are polysilsesquioxanes, hybrids of inorganic oxides and organic network polymers. These amorphous materials are prepared from molecular "building blocks" using sol–gel chemistry, a mild method for the formation of inorganic oxide linkages (Figure 1a).[24-29] The resulting dried xerogels have quite high surface areas (500–1800 m^2/g, BET) that are influenced by the choice of monomer building block, catalyst, and processing conditions. The porosity of the dried xerogel is confined to the low mesopore to micropore domain (<100 Å). We prepared poly(1,4-phenylene)-bridged silsesquioxane by a sol–gel process, described in Figure 1b (BET surface area of **X-1** 1156.42 m^2/g).

* Abstract published in *Advance ACS Abstracts*, September 1, 1994.

(1) Lewis, L. N. *Chem. Rev.* **1993**, *93*(8), 2693.
(2) (a) Wenjiang, N. *Adv. Mater.* **1993**, *5*(7/8), 520. (b) You, J. F.; Papaefthymiou, G. C.; Holm, R. H. *J. Am. Chem. Soc.* **1992**, *114*, 2697. (c) Pocard, N. L.; Alsmeyer, D. C.; McCreery, R. L.; Neenan, T. X.; Callstrom, M. R. *J. Am. Chem. Soc.* **1992**, *114*, 769.
(3) (a) Weller, H. *Angew. Chem., Int. Ed. Engl.* **1993**, *32*, 41. (b) Lifshitz, E.; Yassen, M.; Bykov, L.; Dag, I. *J. Phys. Chem.* **1994**, *98*, 1459.
(4) Henglein, A. *Chem. Rev.* **1989**, *89*, 1861.
(5) (a) Kuczynski, J. P.; Milosavljevic, B. H.; Thomas, J. K. *J. Phys. Chem.* **1984**, *88*, 980. (b) Chan, Y. N. C.; Craig, G. S. W.; Schrock, R. R.; Cohen, R. E. *Chem. Mater.* **1992**, *4*, 885.
(6) Krishran, M.; White, J. R.; Fox, M. A.; Bard, A. J. *J. Am. Chem. Soc.* **1983**, *105*, 7002.
(7) Tricot, Y. M.; Fendler, J. H. *J. Phys. Chem.* **1986**, *90*, 3369.
(8) Kuczynski, J. P.; Thomas, J. K. *J. Phys. Chem.* **1985**, *89*, 2720.
(9) Hernan, P.; Pino, C.; Ruiz-Hitzky, E. *Chem. Mater.* **1992**, *4*, 49.
(10) (a) Spanhel, L.; Arpac, E.; Schmidt, H. *J. Non-Cryst. Solids* **1992**, *147*, 657. (b) Tour, J. M.; Pendalwar, S. L.; Cooper, J. P. *Chem. Mater.* **1990**, *2*, 647. (c) Breitscheidel, B.; Zieder, J.; Schubert, U. *Chem. Mater.* **1991**, *3*, 559.
(11) (a) Zhang, Y.; Raman, N.; Bailey, J. K.; Brinker, C. J.; Crooks, R. M. *J. Phys. Chem.* **1992**, *96*, 9098. (b) Zhang, Y.; Bailey, J. K.; Brinker, C. J.; Raman, N.; Crooks, R. M.; Ashley, C. S. Sol-Gel Optics. *SPIE* **1992**, *1758*, 596.
(12) Kuczynski, J.; Thomas, J. K. *J. Phys. Chem.* **1985**, *89*, 2720.
(13) Colvin, V. L.; Goldstein, A. N.; Alivisatos, A. P. *J. Am. Chem. Soc.* **1992**, *114*, 5221.
(14) Bard, A. J. *Science* **1980**, *207*, 4427.
(15) Takada, T.; Yano, T.; Yasumori, A.; Yamane, M.; Mackenzie, J. D. *J. Non-Cryst. Solids* **1992**, *147*, 631.
(16) Wang, Y.; Suna, A.; Mahler, W. *Mat. Res. Soc. Symp. Proc.* **1988**, *109*, 187.
(17) Wang, Y.; Mahler, W. *Opt. Commum.* **1987**, *61*, 233.
(18) Darwent, J. R.; Porter, G. *J. Chem. Soc., Chem. Commum.* **1981**, 145.
(19) Hoffman, A. J.; Yee, H.; Mills, G.; Hoffman, M. R. *J. Phys. Chem.* **1992**, *96*, 5540.
(20) Weller, H.; Schmidt, H. M.; Koch, U.; Fojtik, A.; Baral, S.; Henglein, A.; Kunath, W.; Weiss, K.; Dieman, E. *Chem. Phys. Lett.* **1986**, *124* (*6*), 557.
(21) Weller, H.; Fojtik, A.; Henglein, A. *Chem. Phys. Lett.* **1985**, *117*(5), 485.
(22) Lukehart, C. M.; Carpenter, J. P.; Milne, S. B.; Burnam, K. J. *CHEMTECH.* **1993**, August, 29.
(23) Wang, Y. *J. Am. Chem. Soc.* **1994**, *116*, 397.
(24) Shea, K. J.; Loy, D. A.; Webster, O. *Chem. Mater.* **1989**, *1*, 572.
(25) Shea, K. J.; Webster, O.; Loy, D. A. Better Ceramics Through Chemistry IV. *MRS Symp. Proc.* **1990**, *180*, 975.
(26) Shea, K. J.; Loy, D.; Webster, O. *J. Am. Chem. Soc.* **1992**, *114*, 6700.
(27) (a) Loy, D. A.; Shea, K. J.; Russic, E. M. Better Ceramics through Chemistry V. *MRS Symp. Proc.* **1992**, *271*, 699. (b) Loy, D. A.; Buss, R. J.; Assink, R. A.; Shea, K. J.; Oviatt, H. W. *Polym. Prepr. (Am. Chem. Soc. Div. Polym. Chem.)* **1993**, *34*, 244. (c) Jamison, G. M.; Loy, D. A.; Shea, K. J. *Chem. Mater.* **1993**, *5*, 1193.
(28) (a) Loy, D. A.; Shea, K. J.; Small, J. H. *J. Non-Cryst. Sol.* **1993**, *160*, 234. (b) Oviatt, H. W., Jr.; Shea, K. J.; Small, J. H. *Chem. Mater.* **1993**, *5*, 943.
(29) Corriu, R. J. P.; Moreru, J. J. E.; Thepot, P.; Wong Chi Man, M. *Chem. Mater.* **1992**, *4*, 1217.

0002-7863/94/1516-9052$04.50/0

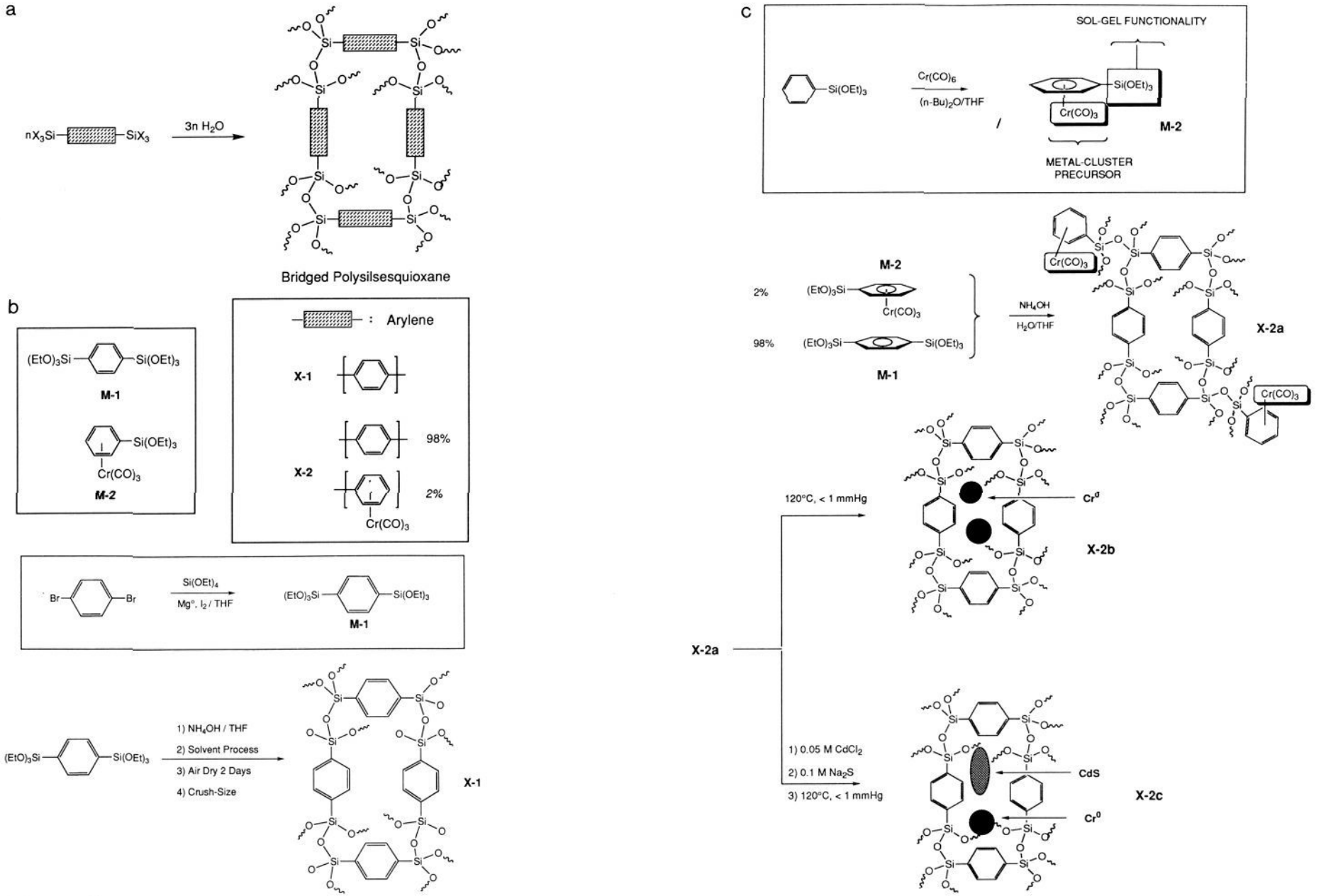

Figure 1. (a) Molecular building block synthesis of polysilsesquioxane and (b), (c) schematic depiction for preparation of **X-1**, **X-2a**, **X-2b**, and **X-2c**.

In previous studies, we have shown that porous polysilsesquioxanes can serve as a confinement matrix for growth of nanosized semiconductor particles.[30,31] Quantum-sized semiconductor particles of CdS ranging from 50 to 90 Å were produced in the pores of these materials. Xerogels prepared from different monomeric building blocks gave rise to CdS particles with different average diameters.

The mild methods used for the synthesis of these xerogels are compatible with a number of organometallic complexes. The sol–gel chemistry used to prepare these hybrid xerogels provides an opportunity to covalently incorporate a number of transition metals in various oxidation states as an integral component of the xerogel matrix.

To illustrate this technique, we describe a strategy for creating small chromium clusters in porous, hybrid xerogel glasses. The nano-sized (<100 Å) chromium metal clusters are introduced by an "internal doping" procedure. The xerogel matrix is prepared by sol–gel processing of 1,4-bis(triethoxysilyl)benzene (**M-1**).[26] The chromium metal precursor, a sol–gel processable $Cr(CO)_3$ arene complex (**M-2**), is covalently incorporated into the polysilsesquioxane by utilizing it as a co-monomer in the sol–gel process. Following hydrolysis–condensation and solvent evaporation, the resulting dried polysilsesquioxane xerogel contains a high internal surface area with pores in the low mesopore to micropore domain (1160.23 m^2/g, BET; 48.84 Å desorption pore diameter). The chromium metal is liberated by heating the xerogel under dynamic vacuum (<1 mmHg, 120 °C). The conditions employed for the xerogel synthesis are compatible with a number of zero-valent transition metal complexes, this approach, therefore, is quite general and may be used for the preparation of a wide variety of dispersed metal clusters in a porous matrix.

We also demonstrate that this procedure can be used for the preparation of complex phases consisting of both semiconductor and transition metal components dispersed in a porous xerogel matrix. This is achieved by combining the internal doping technology with an earlier method that utilized the xerogels as a confinement matrix for semiconductor cluster growth. The strategy is outlined in Figure 1c.

Experimental Section

Syntheses of 1,4-Bis(triethoxysilyl)benzene (M-1) and Chromium Tricarbonyl (Triethoxysilyl)benzene (M-2). 1,4-Bis(triethoxysilyl)-benzene was synthesized from tetraethoxysilane (TEOS) and 1,4-dibromobenzene by a procedure described previously.[26] Hexacarbonylchromium and (triethoxysilyl)benzene were purchased from Aldrich and Hüls Chemical Co., respectively, and tetrahydrofuran (THF) and dibutyl ether was distilled from Na. A solution of hexacarbonylchromium (4 g, 18 mmol) and (triethoxysilyl)benzene (55.5 mL, 230 mmol) in THF/dibutyl ether (1/12 volume ratio) was refluxed under N_2 for 24 h. The sublimed $Cr(CO)_6$ was periodically washed from the condenser with THF/dibutyl ether. The solution was filtered in a dry box under N_2. THF and dibutyl ether were removed in vacuo on a rotary evaporator (10 mmHg, 40 °C bath temperature). Excess (triethoxysilyl)benzene was distilled off at <1 mmHg, 80 °C. SiO_2 flash column chromatography was performed on the residue to separate the product from remaining starting material using a diethyl ether/petroleum ether (10/1: volume ratio) as the mobile phase. The product, isolated by evaporation of the chromatography solvent in 20% yield, is a bright yellow solid. For NMR analysis of **M-2**, samples were transferred to a NMR tube in a dry box: ^1H NMR (500 MHz, $CDCl_3$, TMS) δ 1.28 (t, 9H, J = 6.8 Hz, CH_3), 3.95 (q, 6H, J = 6.8 Hz, $-OCH_2-$), 5.13, 5.55 (tt, 5H, J = 5.8, 8.06 Hz, ArH); ^{13}C NMR (125.8 MHz, $CDCl_3$), δ 18.19, 49.28, 59.38, 89.37, 89.93, 95.52, 99.88; FTIR (film) 2976, 1970, 1889, 1441, 1388, 1283, 1254, 1161, 1074, 1016, cm^{-1}; high-resolution MS calculated for $C_{15}H_{20}O_6CrSi$ 376.0434, observed 376.0438.

Poly(1,4-phenylene)-Bridged Silsesquioxane (Xerogel X-1). Ammonium hydroxide (15 M NH_4OH, 1.9 mL) was added to 1,4-bis-(triethoxysilyl)benzene (**M-1**) (2.01 g, 5 mmol) in THF (22 mL). After shaking, the mixture was transferred to a polyethylene bottle and sealed. Gelation occurred in 5 h. After aging for 3–4 days, the gel was transferred to THF solvent, then broken into small pieces. Solvent processing of the gel was performed by soaking for 2 h each in a series of solvents (THF, CH_2Cl_2, $CHCl_3$, EtOEt, toluene, and CCl_4). After air drying for 2 days, the resulting xerogel was ground to a powder (100–150 μm particle size) and then degassed under vacuum (<1 mmHg) at room temperature.

Xerogels Incorporating the Chromium Tricarbonyl Aryl Group (Xerogels X-2a and X-2b). A solution of 1,4-bis(triethoxysilyl)benzene (**M-1**) (1.97 g, 4.9 mmol) and chromium tricarbonyl(triethoxysilyl)benzene (**M-2**) (0.037 g, 0.1 mmol) was diluted in THF to 23 mL. Ammonium hydroxide (1.9 mL, 15 M NH_4OH) was added, and the solution was shaken, transferred to polyethylene bottle, and then capped. The solution gelled after 1 day. During two additional days of aging, the color of the gel changed to a pale brown-green. The aged gel was solvent processed following the procedure described for **X-1**. After 2 days of air drying the xerogel was ground to 100–150 μm particle size. The powders of the resulting xerogel had a pale brown-green color. The xerogel obtained by this procedure is denoted **X-2a**. **X-2a** was heated at 120 °C for 24 h under a high vacuum (<1 mmHg). After heating, the xerogel darkened somewhat to a green color. This material was denoted **X-2b**. The procedure for preparing these xerogels is represented schematically in Figure 1b.

Xerogels Containing Chromium Metal and CdS Phases (Xerogel X-2c). **X-2a** was prepared by the procedure described above. Cd^{2+} ions were diffused into **X-2a** by first soaking in a 0.05 M $CdCl_2$ ($EtOH-H_2O$, 1/4) solution for 4 days. After washing with water, a solution of 0.1 M Na_2S was added to the dried xerogel. The CdS impregnated xerogel was then heated under high vacuum (<1 mmHg) at 120 °C for 10 h. Figure 1c depicts the preparation of **X-2c**.

Elemental Analysis. Chromium analysis of **X-2b** was performed by Galbraith Laboratories, Inc., Knoxville, TN.

FTIR Analysis. FTIR spectra of **M-2**, **X-2a**, and **X-2b** were obtained on a Precision Scientific RFX-40 FTIR spectrophotometer. The IR of **M-2** showed two intense peaks at 1889.8 and 1968 cm^{-1} consistent with a [$Cr(CO)_3(\eta^6$-arene)] group (Figure 2a). These IR bands have been reported to range between 1970–2000 and 1900–1950 cm^{-1}.[32,33] FTIR spectra of **X-2a** and **X-2b** were obtained from a KBr pellet. Two peaks at 1939.3 and 1990.3 cm^{-1} due to the Cr(CO), carbonyl ($\nu_{C=O}$) are visible in the IR (Figure 2b). After heating under vacuum, these peaks are significantly decreased (Figure 2c).

Solid State NMR. ^{13}C solid state NMR of **X-1** and **X-2a** were obtained using the single pulse method on a Chemagnetics (CMX-200) spectrometer (3 ms contact time). Spinning side bands were identified by their change in chemical shift with a change in spin rate from 2000 to 3000 Hz. ^{13}C solid state NMR of **X-2a** was also obtained by the single pulse method and was compared to the spectra of **X-1**.

TEM, EDAX, and Electron Diffraction. Sample powders of **X-2b** (particle size 100–150 μm) were deposited on a plasma-etched amorphous carbon substrate supported on a copper grid. The transmission micrograph (TEM) images of these xerogels were obtained with a Philips TEM (CM 20/STEM electron microscope). The energy-dispersive X-ray diffraction (EDAX) pattern of chromium metal clusters was also obtained by a Philips EDAX analyzer (TEM-EDAX, PV 9800). The electron diffraction patterns of deposited chromium clusters and chromium clusters coated with CdS were obtained using a 200 kV electron beam. For indexation of the diffraction pattern, the lattice parameters (d values) were calculated by the relationship of $rd = Ll$, where r is a radius of diffraction spot from the center of beam and l is the wavelength of the electron beam (0.025 Å, 200 kV energy). The camera length (L) was calibrated using a gold standard.

DSC and TGA Measurements. Thermal analysis of dried xerogels was performed with a differential scanning calorimeter (DSC) (Du Pont Instruments Model 910) and a thermogravimetric analyzer (TGA) (Du Pont Model 951) under a N_2 atmosphere. All thermal scans were performed using the commercial software of the Thermal Analyst 2000. For DSC measurements an aluminum pan and α-Al_2O_3 standard were used. The N_2 flow rate was held constant during DSC and TGA measurements.

ESR Measurements. The presence of paramagnetic species in **X-2b** was established by a Bruker (ESP 300 E) ESR spectrometer equipped with a Bruker microwave supply (Microwave bridge ER) and a microwave

(30) Choi, K. M.; Shea, K. J. *Chem. Mater.* **1993**, *5*, 1067.
(31) Choi, K. M.; Shea, K. J. *J. Phys. Chem.* **1994**, *98*, 3207.
(32) Zeiss, H.; Wheatley, P. J.; Winkler, H. J. S. *Benzenoid-Metal Complexes*; Ronald Press: New York, 1966.
(33) Sneeden, R. P. A. *Organochromium Compounds*; Academic Press: New York, 1975.

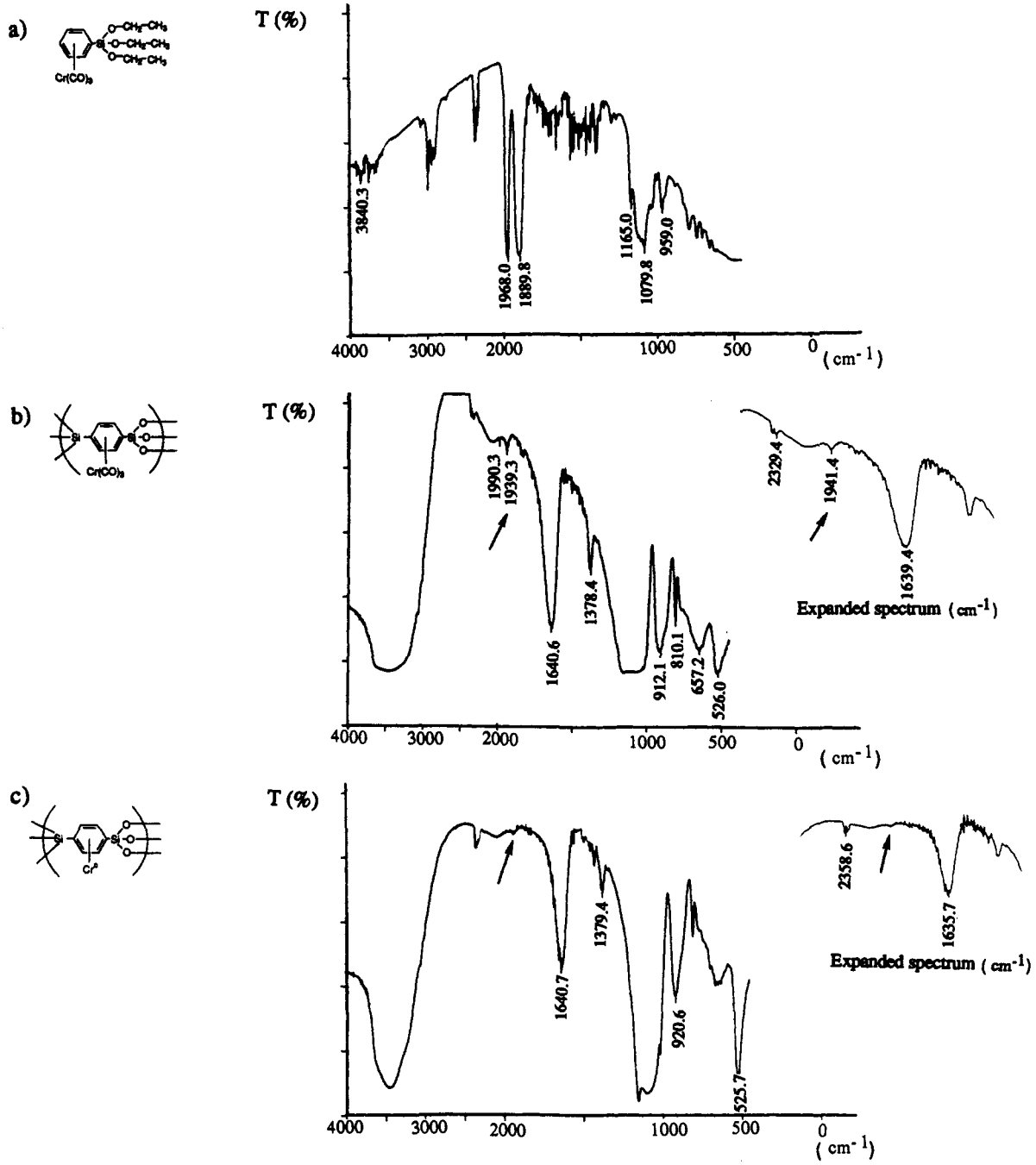

Figure 2. FT-IR results of (a) chromium tricarbonyl (triethoxysilyl)benzene (**M-2**), (b) **X-2a**, and (c) **X-2b**.

frequency counter (HP 5350 B). A powdered sample of **X-2b** in a 5 mm glass ESR tube was scanned at room temperature. DPPH (polycrystalline diphenylpicrylhydrazyl, $g = 2.0036$) was used as a standard.

The g value, ΔH_{pp} (peak-to-peak line width), $\Delta H_{1/2}$ (linewidth at half-height), T (spin–spin relaxation time), and A/B (peak ratio of first-derivative peak) were determined with the following equations:[34]

$$g = h\nu/\beta H_0 \quad (1)$$

$$\Delta H_{1/2} = 2\Delta H_{pp}/2(\ln 2)^{1/2} \quad (2)$$

$$T = h/g\beta\Delta H_{1/2} \quad (3)$$

where β is the Bohr magneton (9.27×10^{-24} J/T) and ν is a microwave frequency applied in this measurement.

Porosity Analysis. Surface area and pore structure analysis was performed from the N_2 adsorption–desorption isotherm by using a Micromeritics (ASAP 2000) porositimeter. Before the measurements, all samples were degassed under high vacuum. Sample amounts of 30–50 mg were used for analysis. The polysilsesquioxane xerogels obtained in this work exhibited a hysteresis loop.[35] The surface areas were calculated from both BET[36] and Langmuir[37] plots. The pore size distribution of xerogels was obtained by the BJH[38] procedure, and pore diameter (d) was calculated from the following relationship:

$$d = 4\sum V_p/\sum A_p \quad (4)$$

where, $\sum V_p$ and $\sum A_p$ are the cumulative pore volume and pore area, respectively. The porosity data for **X-1**, **X-2a**, and **X-2b** are summarized

(34) Rabek, J. F. *Experimental Methods in Polymer Chemistry*; John Wiley and Sons: New York, 1980.

(35) Oscik, J.; Cooper, I. L. *Adsorption*; John Wiley and Sons: New York, 1982.

(36) Brunauer, S.; Emmett, P. H.; Teller, E. J. *J. Am. Chem. Soc.* **1938**, *60*, 309.

(37) Langmuir, I. *J. Am. Chem. Soc.* **1918**, *40*, 1361.

(38) Barrett, E. P.; Joyner, L. G.; Halenda, P. P. *J. Am. Chem. Soc.* **1951**, *73*, 373.

Table 1. Pore Structure Analysis of **X-1**, **X-2a**, and **X-2b** as Determined by Nitrogen Adsorption

	(a) xerogel **X-1**			(b) xerogel **X-2a**			(c) xerogel **X-2b**		
parameters	BET	Langmuir	BJH	BET	Langmuir	BJH	BET	Langmuir	BJH
surface area (m^2/g)	1156.42	1453.18		1160.23	1454.34		963.97	1213.10	
V_m (cm^3/g) at STP	265.65	333.82		266.52	334.08		221.44	278.67	
C	149.82	68.09		141.60	66.69		134.65	63.90	
ΣV_p(ads) (cm^3/g)			0.5005			0.4776			0.4169
ΣA_p(ads) (m^2/g)			418.90			393.25			343.33
d(ads) (Å)			47.79			48.58			48.57
ΣV_p(des) (cm^3/g)			0.3587			0.3770			0.3282
ΣA_p(des) (m^2/g)			330.44			308.73			251.73
d(des) (Å)			43.42			48.84			52.15

in Table 1. In this Table, V_m and C are the volume of sorbent and BET constant (ratio of rate constants for adsorption–desorption), respectively.

Results and Discussion

The preparation of porous xergels *homogeneously* doped with transition metal clusters requires a sol–gel processable source of transition metal. Fortunately, many transition metal complexes are compatible with the mild sol–gel conditions. We have chosen an aryl chromium tricarbonyl complex as a metal source, since these complexes are known to be stable to the mildly acidic or basic conditions used for the sol–gel reactions. The synthesis of chromium tricarbonyl (triethoxysilyl)benzene (**M-2**) from commercially available (triethoxysilyl)benzene and hexacarbonylchromium is shown in Figure 1c. The yellow crystalline complex was isolated and purified by column chromatography.

A xerogel containing 2 mol % chromium tricarbonyl(triethoxysilyl)benzene (**M-2**) in a 1,4-phenylene-bridged polysilsesquioxane matrix was prepared from a 0.2 M solution of **M-1**/**M-2** (98/2 molar ratio) in THF with NH_4OH as catalyst. The solution, initially pale yellow, progressed from a light green to a green-brown after gelation. Following 2 days of aging, the gels were processed by soaking for 2 h each in a series of solvents with decreasing surface tension. Following treatment with the last solvent in the series, CCl_4, the sample was air dried for 2 days.

During this solvent processing, the volume of the gel was greatly reduced, leaving a green-brown, brittle, glassy solid which was ground in a mortar to a powder with a particle size range between 100–150 μm. This xerogel was labeled **X-2a**. For purposes of comparison, poly(1,4-phenylene)-bridged silsesquioxane (**X-1**) was prepared and processed under conditions identical to the previous example, except **M-2** was omitted. ^{13}C solid state NMR of **X-2a** was performed using the single pulse polarization technique, and the results compared with the spectrum of **X-1**. **X-1** shows a single ^{13}C adsorption peak at 134.27 ppm. The two aromatic sp^2 resonances in the monomer **M-1** (134.36 and 133.45 ppm) are separated by only 1 ppm. The peak width of the ^{13}C adsorption in the solid state NMR of **X-1** is >5 ppm and appears to be a broad singlet centered at 133.6 ppm. The ^{13}C NMR of **X-2a** shows a main peak at 134 ppm with two shoulders at 129 and 138 ppm. The ^{13}C sp^2 resonances arising from the chromium complexed arene group are observed at approximately 90 ppm. The shoulders of the main peak observed in the ^{13}C of **X-2a**, at 129 and 136 ppm, are not observed in **X-1** and may be due to the presence of chromium bisaryl complexes, since the chemical shifts reported for these species fall in the range observed for these new adsorptions.[39]

The dried xerogel **X-2a** was heated at 120 °C under high vacuum for 24 h to liberate CO and chromium atoms. The color of resulting xerogel darkened somewhat during heating. This xerogel was labeled **X-2b**. Elemental analysis of **X-2b** indicates 0.68 wt % chromium.

A distribution of irregularly shaped dark features was observed in the TEM image of **X-2b** (Figure 3). The dark features, indicated by arrows, are distributed throughout the matrix. These

(39) Graves, V.; Lagowski, J. J. *Inorg. Chem.* **1976**, *15*, 577.

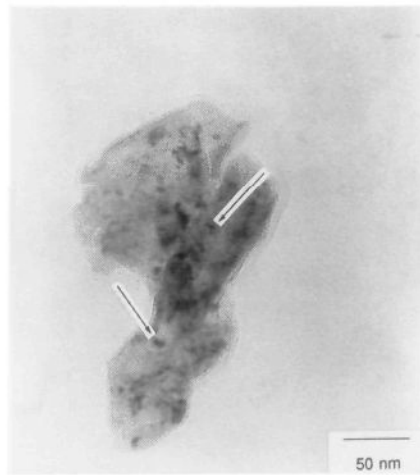

Figure 3. TEM image of **X-2b**. The bright matrix is a polysilsesquioxane glassy material and dark spots (arrows) are the crystalline chromium metal clusters.

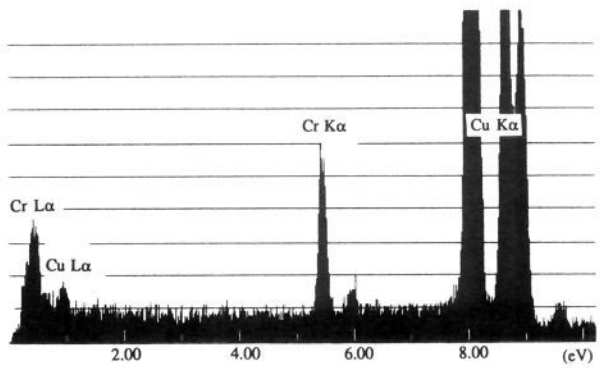

Figure 4. EDAX pattern from the dark features in **X-2b**.

phases are absent in the TEM image of **X-1**. The dark images vary considerably in size, but most have diameters <100 Å. The identity of these features was established by EDAX and electron diffraction techniques. Figure 4 shows an EDAX pattern obtained by focusing on a single dark image in the TEM. In the EDAX pattern, the characteristic Kα and Lα peaks for chromium were observed. The Cu (Kα, Lα) peaks in Figure 4 arise from the Cu grid of the sample holder. Additional information regarding these clusters, in particular their crystallinity, was obtained from the electron diffraction pattern. Figure 5 shows the diffraction pattern of a single dark image in the TEM (200 kV electron beam). The indexed diffraction pattern allows assignment of the chromium as microcrystallites of cubic structure with a lattice parameter (a) of 2.8839 Å.

Some insight into the sequence of events leading to formation of the chromium metal clusters was obtained from a DSC/TGA investigation of **X-2a**. DSC analysis was carried out over a *temperature range of 25–600 °C using* α-Al_2O_3 *standard under* N_2 atmosphere. For comparison, the thermal behavior of **X-1**

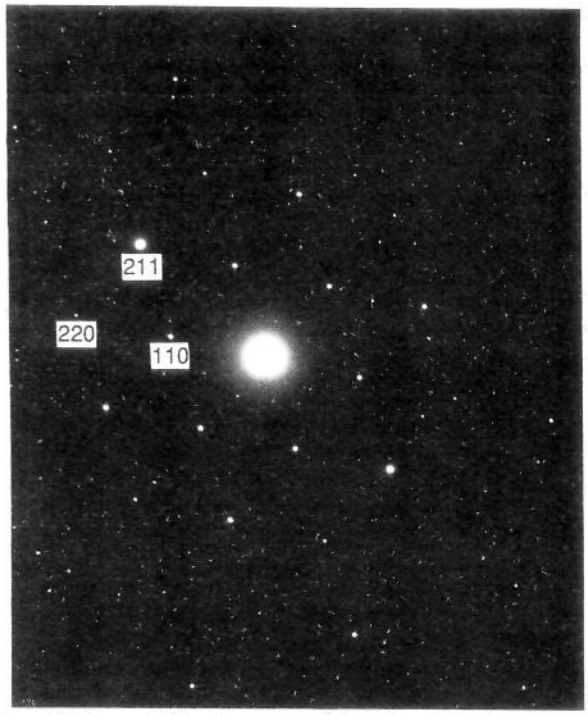

Figure 5. Electron diffraction pattern of chromium clusters prepared in **X-2b**. It shows a chromium single crystalline pattern of cubic. Each spot is identified as {110}, {211}, and {220} planes. Zone axis is [111].

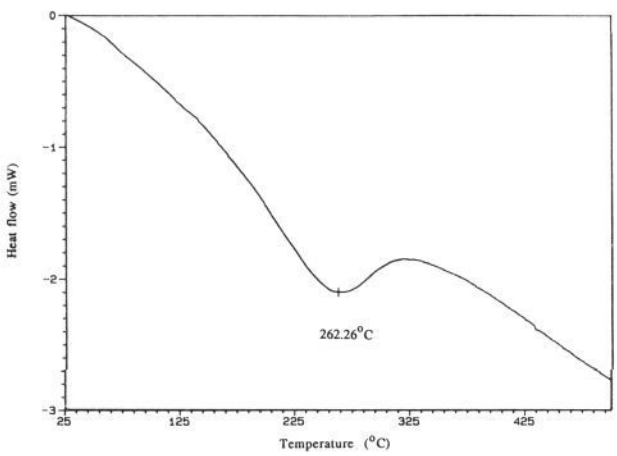

Figure 6. DSC measurements of **X-2a**.

(no chromium complex) is also taken. Both xerogels exhibit an endotherm at approximately 150 °C (scan rate 10 °C/min), which can be attributed in part to desolvation and perhaps some condensation of residual SiOH linkages. It also corresponds to the range of temperatures at which (aryl)tricarbonylchromium complexes decompose.[40] Following heating to 150 °C, both samples were cooled and then heated a second time. It was then observed that the xerogels no longer exhibited the endotherm at approximately 150 °C. In addition to the endotherm at 150 °C, **X-2a** exhibited a second endothermic peak with an onset temperature of 262 °C (Figure 6). This peak is absent in the DSC trace of the xerogel lacking the chromium monomer (**X-1**). One possible explanation for the origin of the high-temperature endotherm in the DSC curve is that it arises from decomposition of bis(η^6-arene)chromium complexes which could be the primary decomposition products of the (η^6-arene)chromium tricarbonyl complex. This suggestion is supported by the report that the monomeric brown bis(η^6-arene)chromium(0) complex [$Cr(C_6H_6)_2$] has a melting/decomposition point of 280 °C.[40]

(40) Timms, P. L. *J. Chem. Educ.* **1972**, *49*, 782.

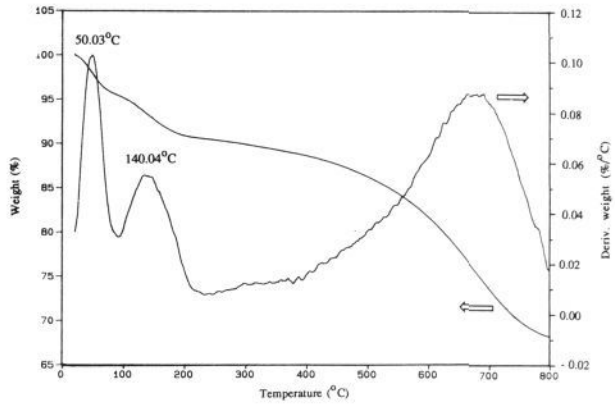

Figure 7. TGA curve and derivative plot of **X-2a**.

Scheme 1

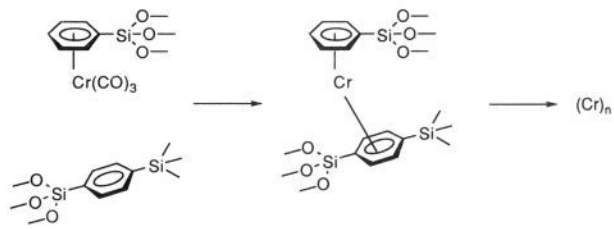

A possible mechanism for the chromium metal deposition would then involve initial loss of CO followed by formation of a bis-(η^6-arene)chromium(0) complex (Scheme 1). The reported range of decomposition temperatures for bis(η^6-arene)chromium(0) tricarbonyl complexes are from 110–175 °C. Since this falls within the temperature range of desolvation and condensation that is characteristic of all xerogels, unambiguous assignment is difficult. However, the observation of the second endotherm in **X-2a** supports this analysis. Decomposition of the bis-arene complex (262 °C) precedes formation of chromium (0) clusters. The lower decomposition temperature of the bis(η^6-arene)-chromium(0) complexes from those reported in the literature could arise from the fact that the arene groups in the highly condensed matrix have diminished mobility and flexibility. This could result in the formation of bis(η^6-arene)chromium(0) complexes in non-ground state geometries. These *distorted* complexes would be expected to have decomposition temperatures lower than similar complexes in their ground conformational states (Scheme 1).

We note however that the conditions of the DSC experiment differ from those used to deposit the Cr metal clusters in **X-2**. The correspondence of this mechanistic picture to decomposition under dynamic vacuum at lower temperatures remains to be established.

Figure 7 also shows a TGA curve of **X-2a** and its derivative plot. The first weight loss, characteristic of all polysilsesquioxane xerogels, is attributed to loss of solvent. The second weight loss step occurs from 100 to 200 °C. This is consistent with the DSC result and could arise from both dehydration and the dissociation of the carbonyl groups. The temperature of this weight loss corresponds to the decomposition temperature of (aryl)chromium tricarbonyl derivatives (130 to 200 °C).[41] Relatively little weight loss is found beyond the second region until temperatures rise above 450 °C.

Evaluation of the porosity of dried polysilsesquioxane xerogels (**X-1** and **X-2**) was performed by analysis of the N_2 adsorption–desorption isotherm. The surface area of xerogels was calculated by both BET[36] and Langmuir[37] methods, and pore size was obtained by the BJH[38] method. The cumulative pore volume and pore area plots and the pore volume and pore area distribution

(41) Wilkenson, S. G. *Comprehensive Organometallic Chemistry*; Pergaman Press, Inc.: New York, 1982; Vol. 3.

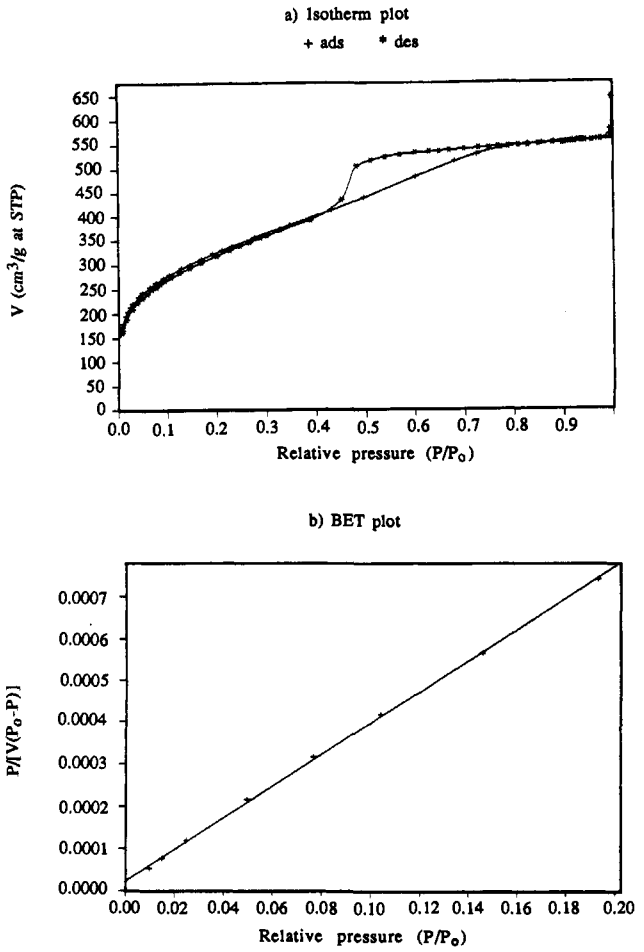

Figure 8. (a) Adsorption–desorption isotherm and (b) BET plots of **X-1**.

curves of **X-1** and **X-2** were also obtained as a function of pore diameter. A typical isotherm plot and pore volume and pore area distribution plots are given in Figures 8 and 9, and the derived parameters are listed in Table 1. The N_2 adsorption–desorption isotherm plot of **X-1** shows a hysteresis loop which suggests a pore shape with bottle-neck restrictions.[35] The BET and Langmuir plots of **X-1** yield surface areas of 1156 and 1453 m^2/g, respectively.

The pore volume and area distribution curves for **X-1** (Figure 9) exhibit a maximum at a diameter of 36 Å. From eq 4, a pore diameter from the desorption curve of **X-1** was calculated to be 43 Å. Isotherm plots of **X-2a** and **X-2b** show a similar hysteresis loop to that obtained for **X-1**. Surface areas of **X-2a** and **X-2b** are listed in Table 1. The pore volume and pore area distribution curves of **X-2a** and **X-2b** also show single sharp peaks at 36 Å, similar to that shown by **X-1**.

Poly(1,4-phenylene) bridged silsesquioxane xerogels are porous materials with high surface areas and average pore sizes in the low mesopore to micropore range. The similarity of **X-1** and **X-2a** xerogels with respect to surface area and pore size suggests that incorporation of **M-2** (2%) in the sol–gel formulation causes no significant changes in the gross morphology of the resulting xerogel. A comparison of the data for **X-2a** and **X-2b** (Table 1), reveals a slight decrease (17%) in surface area following chromium deposition. This slight decrease in surface area can arise from coverage of the inner surface of the xerogel matrix with deposited chromium clusters. For comparison, the surface areas of **X-1** before and after heating at 120 °C were determined. No change (±1%) in surface area was observed. In addition to a change in surface area, chromium deposition results in only a slight increase in the average pore size. The calculated values for the pore diameter of **X-1**, **X-2a**, and **X-2b** were found to be 43.42, 48.84, and 52.15 Å, respectively. Thus, chromium metal deposition (0.68% by weight) produced no significant change in the pore diameter of the xerogel. This establishes that the chromium clusters reside in an open porous xerogel and should be accessible to external reagents and substrates.

Table 2. ESR Parameters of Chromium Clusters Doped into **X-2b**

ESR parameters	xerogel-**2b**
g value	1.985
ΔH_{pp} (G)	400.39
A/B peak ratio	0.91
T (s)	1.26×10^{-10}
$\Delta H_{1/2}$ (G)	471.42

No precautions were taken during processing and storage of the xerogels to exclude oxygen. The darkening of **X-2b** suggests possible oxidized forms of chromium during their preparation. To establish the presence of paramagnetic chromium species that could be present in the xerogel, ESR measurements were performed. A single ESR peak in **X-2b** was obtained from a powder sample at a microwave frequency of 9.439 GHz. The ESR peak of **X-2b** exhibited a Gaussian-type curve determined from the ratio of the peak slopes. The calculated ESR parameters of **X-2b** are listed in Table 2. A g value of 1.985 in **X-2b** may arise from either oxidized chromium impurities[42] or $[Cr(\eta^6\text{-arene})_2]^+$ complexes[43] since both have g values close to the observed g value in **X-2b**. Efforts to identify oxides of chromium using XPS have so far proven unsuccessful due to excessive charging of the sample. The lattice parameter (a = 2.8839 Å) obtained from the electron diffraction pattern is consistent with cubic microcrystallites of chromium metal and *not* that of the oxides of chromium. This is consistent with the bulk of the metal in the zero-valent state but does not rule out some fraction of surface oxidation of the particles.

Semiconductor/Transition Metal Cluster Nanocomposites. Heterogeneous mixtures of transition metal and semiconductor clusters have considerable potential as catalysts. A number of interesting reactions of small molecules with these heterogeneous transition metal clusters have been reported.[1] We have previously reported that amorphous polysilsesquioxanes can be used as a confinement matrix for the growth of quantum-sized CdS semiconductor particles.[30] The preceding results establish that nano-sized chromium clusters may be prepared in a porous polysilsesquioxane matrix by internal doping. We have been able to combine these two technologies to produce porous materials that contain intimate nanocomposites of cadmium sulfide and chromium metal. Xerogel **X-2a** was prepared as described above. The air-dried (but not heated) **X-2a** was then soaked in a 0.05 M aqueous solution of $CdCl_2$ for 4 days. Following washing and air drying, it was then soaked in a solution of 0.1 M Na_2S. Following drying in a vacuum oven, the xerogels were heated at 120 °C under high vacuum for 10 h to deposit chromium(0) metal. The EDAX spectra of several dried xerogels revealed chloride peaks; these were eliminated by soaking the material in water for several hours. The resulting xerogel, labeled **X-2c**, was analyzed as described previously for **X-2b**. Figure 10 shows a TEM image of **X-2c**. The image shows two distinct phases distributed in the matrix.

The dark phase was identified as chromium crystallites (cubic structure) from both EDAX and electron diffraction results obtained by focusing on a dark area in the image. In addition, the light phases surrounding the dark areas were identified as CdS by both EDAX and electron diffraction techniques. The TEM images confirm that the chromium metal and CdS phase

(42) Kazanski, V. B.; Turkovich, J. *J. Catal.* **1967**, *8*, 231.
(43) Gold, B.; Linder, W. B. *J. Am. Chem. Soc.* **1979**, *101*, 22.

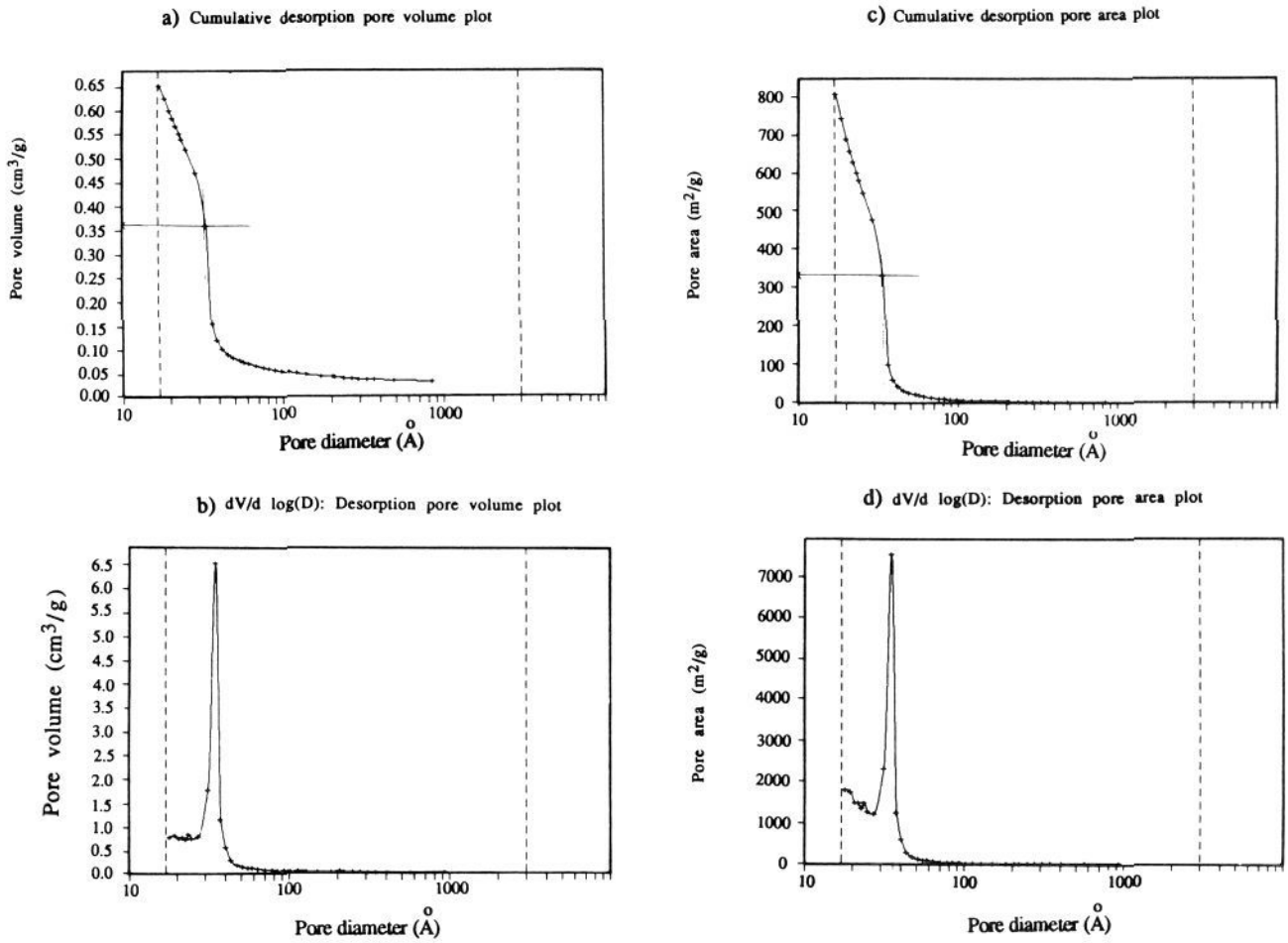

Figure 9. (a) The desorption cumulative pore volume and (c) cumulative pore area plots of **X-1**; (b) the desorption pore volume and (d) pore area distribution curves of **X-1**.

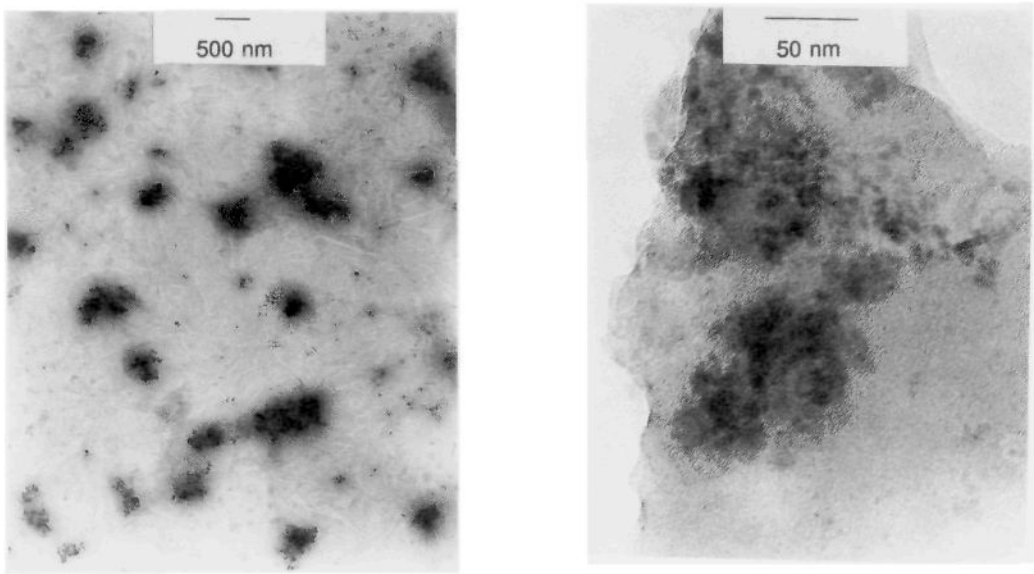

Figure 10. TEM images of chromium clusters coated with CdS prepared in **X-2c**. In two distinct cluster phases, dark and light phases are identified to be chromium and CdS phases, respectively.

coexist in the polysilsesquioxane matrix. The shading, rather that discrete particles revealed by the TEM, suggests a different morphology for this composite material than that obtained for either homogeneous CdS or chromium metal doped materials. Figure 11 shows the EDAX pattern of the chromium composite/CdS phases in **X-2c**. When the electron beam is focused on an area of approximately 30 Å, it shows Cd (Lα), S (Kα), Si (Kα), Cu (Kα, Lα), and Cr (Kα) peaks. The diffraction pattern reveal characteristics of microcrystalline CdS (cubic) and chromium (cubic). (Peaks attributed to Cu are due to the Cu grid.) The presence of surface oxidized chromium and CdS is not excluded by these observations. We note however that, in a related XPS study of CdS doped xerogels, no oxidized sulfur was observed.[44]

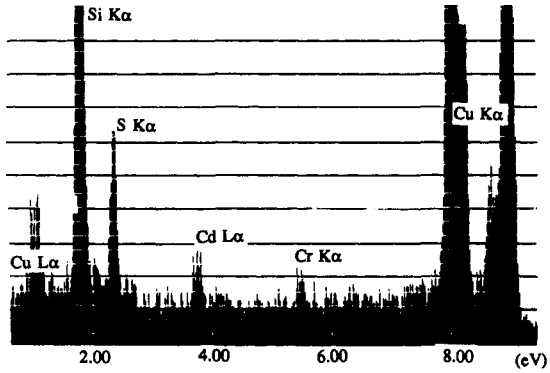

Figure 11. EDAX pattern of chromium clusters coated CdS in **X-2c**.

Conclusions

Nano-sized chromium metal clusters were grown in a porous polysilsesquioxane matrix by a novel "internal doping" procedure. The chromium precursor consists of a sol–gel processable zerovalent arene tricarbonyl chromium complex which was used as an integral component of the polysilsesquioxane matrix. Heating the dried xerogel under a vacuum decomposes the chromium tricarbonyl complex and deposits nano-sized chromium clusters in the porous xerogel. Analysis of the electron diffraction pattern established that the irregularly shaped chromium particles are present as microcrystallites dispersed in the polysilsesquioxane matrix. Little change in surface area and pore size of the xerogel as a result of internal doping of chromium clusters was found. This technique provides a method for producing stable nano-sized transition metal clusters in a solid porous xerogel matrix. The average pore sizes of the xerogels are <50 Å. In addition, two intimate phases consisting of CdS and chromium were also prepared in a porous xerogel by first doping CdS into the material followed by heating at 120 °C under high vacuum. Verification of the identity of the mixed phases was directly revealed by TEM, EDAX, and electron diffraction results. The possible applications of these materials for use as size selective heterogeneous catalysts are currently being explored.

(44) Shea, K. J.; Choi, K. M.; Hemminger, J. Manuscript in preparation.

Acknowledgment. We thank Prof. M. L. Mecartney for helpful discussions regarding TEM and electron diffraction patterns. We also thank Dr. Jejun Wu for assistance with the solid state NMR and ESR measurements. This work was financially supported by grants from National Science Foundation (Division of Materials Research) and the Air Force Office of Scientific Research.